In vitro and in vivo investigations into the carbene gold chloride and thioglucoside anticancer drug candidates NHC-AuCl and NHC-AuSR

Walther W., Dada O., O'Beirne C., Ott I., Sanchez-Sanz G., Schmidt C., Werner C., Zhu X., Tacke M.

Letters in Drug Design & Discovery
2017 ; 14(2): 125-134
2016 (first published online)
doi: 10.2174/1570180813666160826100158

Publisher: Bentham Science Publishers

Letters in Drug Design & Discovery, 2017, *14*, 125-134

RESEARCH ARTICLE

In Vitro and *In Vivo* Investigations into the Carbene Gold Chloride and Thioglucoside Anticancer Drug Candidates NHC-AuCl and NHC-AuSR

Wolfgang Walther[a,b], Oyinlola Dada[c], Cillian O'Beirne[c], Ingo Ott[d], Goar Sánchez-Sanz[c], Claudia Schmidt[d], Carsta Werner[e], Xiangming Zhu[c] and Matthias Tacke[c,*]

[a]*Max Delbrück Center (MDC) for Molecular Medicine, Robert-Rössle-Str. 10, D-13125 Berlin, Germany;* [b]*Experimental and Clinical Research Center, Charité, Lindenberger Weg 80, D-13125 Berlin, Germany;* [c]*School of Chemistry, University College Dublin, Belfield, Dublin 4, Ireland;* [d]*Institute of Medicinal and Pharmaceutical Chemistry, Technische Universität Braunschweig, Beethovenstr. 55, D-38106 Braunschweig, Germany;* [e]*EPO GmbH Berlin-Buch, Robert-Rössle-Str. 10, D-13125 Berlin, Germany*

ARTICLE HISTORY

Received: June 20, 2016
Revised: August 18, 2016
Accepted: August 22, 2016

DOI:
10.2174/1570180813666160826100158

Abstract: The anticancer drug candidate 1,3-dibenzyl-4,5-diphenyl-imidazol-2-ylidene gold(I) chloride (NHC-AuCl) and its 2',3',4',6'-tetra-O-acetyl-β-D-glucopyranosyl-1'-thiolate derivative (NHC-AuSR), which is a potential ligand for glucose transporters, were tested on the NCI 60 cancer cell panel *in vitro*. NHC-AuCl and NHC-AuSR showed very good activity against a wide range of human cancer cell lines inclusive renal cell cancer with similar average GI50 values of 1.78 and 1.95 μM, respectively. This encouraged maximum tolerable dose (MTD) experiments in mice, where MTD values of 10 mg/kg for NHC-AuCl and 7.5 mg/kg for NHC-AuSR were determined with single injections to groups of 2 mice. In the following tumor xenograft experiment NHC-AuCl and NHC-AuSR were given at MTD in 6 injections to two cohorts of 6 CAKI-1 tumor-bearing NMRI:nu/nu mice, while a control cohort of 6 mice was treated with solvent only. NHC-AuCl at the dose of 10 mg/kg and NHC-AuSR at the lower dose of 7.5 mg/kg induced both low toxicities in the form of abdominal swelling but no significant body weight loss was seen in both groups. The tumor volume growth reduction was significant and almost identical; optimal T/C values of 0.47 were observed on day 19 for NHC-AuCl and on day 29 for NHC-AuSR. Immunohistochemistry for the proliferation marker Ki-67 and the angiogenesis marker CD31 did not show significant changes due to NHC-AuCl or NHC-AuSR treatment in the animals. However, thioredoxin reductase (TrxR) inhibition with IC50 values of 1.5 μM for NHC-AuCl and 3.1 μM for NHC-AuSR seems to indicate that apoptosis induction through elevated oxidative stress is the main mechanism for the two gold compounds.

Keywords: Carbene-gold anticancer drug, NCI 60 cancer cell panel, thioredoxin reductase, CAKI-1 renal cell cancer, xenograft mouse model, glucose transporter.

INTRODUCTION

Renal-cell carcinoma (RCC) is the most common malignant disease of the adult kidney, which accounts for approximately 3% of adult malignancies [1]. If not detected early, these cancers develop to an invasive adenocarcinoma, which have very limited treatment options and poor outcomes. New targeted compounds like Bevacizumab, Sunitinib, Sorafenib, Temsirolimus and others give a certain amount of hope to patients with advanced renal-cell cancer, since these compounds can block the VEGF or mTOR pathway and are therefore anti-angiogenic [2]. Nevertheless, these new drugs cannot cure advanced or metastatic renal cell cancer and give the patient only a few extra months of survival. These clinical facts suggesting new therapeutic regimens must be explored in the quest to develop an effective therapy for these metastatic or advanced forms of renal-cell cancer.

There is significant unexplored space for chemotherapeutic coinage metal-based drugs [3] targeting difficult to treat cancers like RCC. Already in 2008 a paper by Youngs suggested that carbene-silver acetato complexes derived from 4,5-dichloro-imidazole may have the stability and antitumoral activity to become anticancer drug candidates [4]. The idea was further pursued and led to the development of more lipophilic benzyl-substituted imidazole- and benzimidazole-derived carbene-silver, -gold, and -ruthenium complexes showing activity against the human renal cancer line CAKI-1 [5-23]. So far, the most promising derivative 1-methyl-3-(*p*-cyanobenzyl)benzimidazole-2-ylidene silver(I) acetate (SBC1) showed activity against CAKI-1 cells with an

*Address correspondence to this author at the School of Chemistry, University College Dublin, Belfield, Dublin 4, Ireland; Tel: 00353-1-7168428; E-mail: matthias.tacke@ucd.ie

1875-628X/17 $58.00+.00

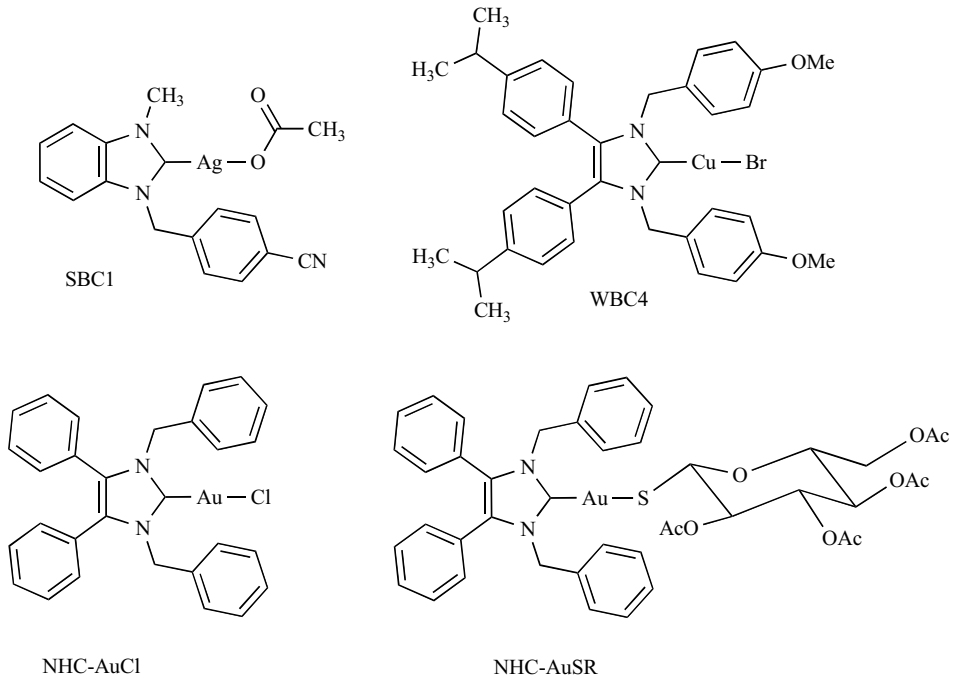

Fig. (1). Molecular structure of the carbene-metal compounds SBC1, WBC4, NHC-AuCl and NHC-AuSR.

IC50 value of 1.2 μM [20], which is superior when compared to cisplatin. Due to its lipophilicity and suitable shape, the anticancer drug candidate SBC1 binds well to albumin and interacts with DNA *in vitro*, but failed to show an antitumoral effect *in vivo* [24]. However, further synthesis led to 1,3-di(*p*-methoxybenzyl)-4,5-di(*p*-isopropylphenyl)-imidazol-2-ylidene copper(I) bromide (WBC4), which shows nanomolar activity with an IC50 value of 0.65 μM against CAKI-1 cells [25] and a significant antitumoral effect against renal-cell cancer *in vivo* [26].

This paper is now investigating the anti-proliferative effect of the two carbene-gold anticancer drug candidates; gold derivatives are known for showing an interesting apoptosis mechanism targeting mitochondria [27] *via* thioredoxin reductase (TrxR) inhibition [28]. So, 1,3-dibenzyl-4,5-diphenyl-imidazol-2-ylidene gold(I) chloride (NHC-AuCl) and its 2',3',4',6'-tetra-O-acetyl-beta-D-glucopyranosyl-1'-thiolate derivative (NHC-AuSR) [11], which might be transported by overexpressed glucose transporters [29] selectively into cancer cells, are tested against the full panel of NCI 60 cancer cell lines *in vitro* as well as for their activity and toxicity in a CAKI-1 xenograft mouse model *in vivo*. In addition, both gold derivatives are tested as TrxR inhibitors and NHC-AuSR as a potential glucose transport binder; the structures of SBC1, WBC4, NHC-AuCl and NHC-AuSR are shown in Fig. **1**.

MATERIALS AND METHODS

Cell Assays

The cell viability tests were performed on the US National Cancer Institute's 60 cancer cell panel (NCI 60) at Frederick, MD. For these tests both gold compounds were formulated in DMSO:glycerol 9:1 and given to the cells at concentrations ranging from 10 nM to 10 μM. The growth inhibition assay allows for a 48 h incubation period with drug candidate solutions and uses Sulforhodamine B (SRB) to measure drug-induced cytotoxicity as described before [30]. The interpretation of the data is based on GI50 values, which are concentrations required to inhibit cell growth by 50%.

CAKI-1 Xenograft

In a first animal experiment the maximum tolerable dose (MTD) of NHC-AuCl and NHC-AuSR was determined in female NMRI:nu/nu mice. Both compounds were dissolved in DMSO (final concentration 10%) and further diluted with 5% Tween 80 in saline. For better comparison both compounds were given equimolar, so that NHC-AuSR (molecular weight of 961 g/mol) is given with 1.5-fold dosing compared to NHC-AuCl (molecular weight of 633 g/mol). Female NMRI:nu/nu mice (n=2 mice per group) were treated with 1, 5, 10 and 20 mg/kg (NHC-AuCl) or 1.5, 7.5, 15 and 30 mg/kg (NHC-AuSR) intraperitoneally (i.p.) in single injections of 0.1 ml in order to determine the approximate MTD. In this experiment maximum body weight loss and side effects were documented.

In the second *in vivo* experiment 1 x 10^7 CAKI-1 cells (expanded *in vitro* in McCoy´s medium + 10% fetal bovine serum) were injected subcutaneously (s.c.) in a volume of 0.1 ml to female NMRI:nu/nu mice (n=6 mice per group) on day 0. When tumors were grown to a palpable size of around 0.1 cm^3 mice were randomised and treatment was initiated on day 7. For groups B and C the experimental anticancer drug NHC-AuCl (group B) and NHC-AuSR (group C) were injected into mice i.p. at doses of 10 (group B) or 7.5 (group C) mg/kg on days 7, 11, 15, 22, 25 and 28, while the control group (group A) of mice was treated with the solvent only. Tumor size was measured with a caliper instrument. Tumor

volumes, relative tumor volumes (relation to the first treatment day) and treated to control (T/C) values were calculated. Body weight and lethality of the mice were determined continuously during the experiments to estimate tolerability of the drug. Mice were sacrificed 7 days after their last treatment and necropsy was performed for evaluation of side effects. Tumors were removed and snap frozen for immunohistochemical analyses.

The animal experiments were performed according to the German Animal Protection Law and with approval from the responsible local authorities (Berlin, Germany). The *in vivo* procedures were consistent and in compliance with the UKCCCR guidelines.

Ki-67 and CD31 Immunohistochemistry

Sections from snap frozen Caki-1 tumors (6 per group, thickness 5 µm) were fixed with 3.7% paraformaldehyde, blocked with H_2O_2 and goat serum. After incubation with the primary antibody (rat anti-mouse CD31, clone: MEC13.3, BD Pharmingen, Heidelberg, Germany), slides were incubated with a secondary HRP-labelled goat anti-rat antibody (Jackson ImmunoResearch, Hamburg, Germany), DAB substrate (Dako, Hamburg, Germany) and counterstained with hematoxylin. Evaluation of microvessel density was performed with AxioVision 4.5 (Zeiss, Jena, Germany). Vessels were labelled in six representative pictures of each tumor and quantified for microvessel size, number and ratio (microvessel area vs. total tumor area).

For the staining of the Ki-67 proliferation marker, fixation and blocking was performed according to the procedure used for CD31. The slides were incubated with the primary mouse anti-human Ki-67 antibody (Dako; clone: MIB-1). As secondary antibody the HRP-labelled anti-mouse antibody was used. For the staining the DAB substrate and for counterstaining hematoxylin were used (Dako). For evaluation of Ki-67 expression 6 pictures of each tumor were taken and the number of positive vs. negative cells was counted in three fields of view.

STATISTICAL ANALYSIS

Statistical evaluation for all experiments was performed with the One-way Anova test and Bonferroni-correction. The level of statistical significance was defined with a p-value of $p \leq 0.05$.

Inhibition of Mammalian TrxR

To determine the inhibition of mammalian TrxR an established microplate reader based assay was performed. For this purpose, commercially available rat liver TrxR (from Sigma-Aldrich) was used and diluted with distilled water to achieve a concentration of 3.58 U/mL. The compounds, NHC-AuCl and NHC-AuSR, were freshly dissolved as stock solutions in DMF. 25 µL aliquots of the enzyme solution and 25 µL of either potassium phosphate buffer pH 7.0 containing the compounds in graded concentrations or 25 µL buffer without compounds but DMF (positive control) were added. 50 µL of a blank solution (DMF in buffer) was also prepared (final concentrations of DMF: 0.5% V/V). The resulting solutions were incubated with moderate shaking for 75 min at 37°C in a 96-well plate. To each well, 225 µL reaction mixture (1 mL reaction mixture consists of 500 µL potassium phosphate buffer pH 7.0, 80 µL EDTA solution (100 mM, pH 7.5), 20 µL BSA solution (0.2%), 100 µL of NADPH solution (20 mM) and 300 µL distilled water) were added and the reaction started immediately by addition of 25 µL of 20 mM ethanolic DTNB solution. After proper mixing, the formation of 5-TNB was monitored with a microplate reader at 405 nm 10 times in 35 s intervals for about 6 min. The increase in 5-TNB concentration over time followed a linear trend ($r^2 \geq 0.990$), and the enzymatic activities were calculated as the slopes (increase in absorbance per second) thereof. For each tested compound, the noninterference with the assay components was confirmed by a negative control experiment using an enzyme-free test solution. The IC50 values were calculated as the concentration of compound decreasing the enzymatic activity of the untreated control by 50% and are given as the means and error of three repeated experiments.

Computational Details

All compounds have been optimized at the B3LYP [31, 32] computational level with the 6–31+G(d) basis set [33] applied to the lighter elements inclusive sulfur. The LANL2DZ basis set [34] is used throughout for the heavier elements of copper and gold. Frequency calculations have been performed at the same level in order to confirm that the structures obtained correspond to energetic minima. The effect of water solvation was then accounted for using the SCFR-PCM approach implemented in the Gaussian09 [35] package including dispersing, repulsing and cavitation energy terms of the solvent in the optimisation.

A molecular docking study was undertaken using the AutoDock Vina 1.1.2 [36] modelling software. The structures were imported into the AutoDock Vina 1.1.2 modelling software. The Human Glucose Transporter (GLUT1) structure was taken from crystal structure PDBID 4PYP [37], while NHC-M-thioglucoside ligands structures (M = Au or Cu) were taken from the optimised geometry at quantum level. AutoDockTools 1.5.6 was used for establishing the Autogrid points as well as visualization of docked ligand–transporter structures. The target site on the NHC-M-glucoside was specified to encompass the entire inner region of the human glucose transporter, GLUT1, site. Further, the grid center was also established by centering the grid box on the GLUT1.

RESULTS AND DISCUSSION

In vitro Efficacy of NHC-AuCl and NHC-AuSR

NHC-AuCl and NHC-AuSR were tested against 6 leukemia, 8 NSC lung, 7 colon, 5 CNS, 8 melanoma, 6 ovarian, 7 renal, 2 prostate and 4 breast cancer cell lines. The concentrations that inhibited cell growth by 50% (GI50, as determined by a SRB assay after a 48 h incubation period) were generally in the single digit micromolar range with NHC-AuCl and NHC-AuSR exhibiting average GI50 values of 1.78 and 1.95 µM, respectively. NHC-AuCl exhibited its

Table 1. Overview on results obtained in cytotoxicity tests of NHC-AuCl against the NCI 60 cancer cell line panel; efficacy is shown as growth inhibition 50% (GI50) values.

Cell Line	GI50 [M]	Cell Line	GI50 [M]
Leukemia			
CCRF-CEM	1.36E-6	**NSC Lung Cancer**	
HL-60(TB)	1.44E-6	A549/ATCC	7.28E-6
K-562	6.08E-7	HOP-62	1.99E-6
MOLT-4	2.72E-6	HOP-92	1.57E-6
RPMI-8226	1.15E-6	NCI-H226	1.04E-5
SR	3.19E-7	NCI-H23	1.89E-6
		NCI-H322M	2.28E-6
		NCI-H460	2.37E-6
		NCI-H522	1.39E-6
Colon Cancer			
COLO 205	2.04E-6		
HCC-2998	1.77E-6	**CNS Cancer**	
HCT-116	1.59E-6	SF-268	1.86E-6
HCT-15	1.35E-6	SF-295	3.82E-6
HT29	1.80E-6	SNB-19	1.65E-6
KM12	2.60E-6	SNB-75	1.29E-6
SW-620	1.76E-6	U251	1.55E-6
Melanoma			
LOX IMVI	1.27E-6		
MALME-3M	1.71E-6	**Ovarian Cancer**	
M14	1.69E-6	IGROV1	1.81E-6
MDA-MB-435	1.66E-6	OVCAR-3	1.66E-6
SK-MEL-2	1.78E-6	OVCAR-4	1.37E-6
SK-MEL-5	1.72E-6	OVCAR-8	1.96E-6
UACC-257	1.65E-6	NCI/ADR-RES	3.49E-6
UACC-62	1.61E-6	SK-OV-3	2.54E-6
		Prostate Cancer	
Renal Cancer		PC-3	1.84E-6
786-0	1.44E-6	DU-145	1.83E-6
A498	1.77E-6		
CAKI-1	1.74E-6	**Breast Cancer**	
RXF 393	1.55E-6	MCF7	1.31E-6
SN12C	1.86E-6	HS 578T	2.40E-6
TK-10	1.78E-6	BT-549	1.66E-6
UO-31	1.62E-6	MDA-MB-468	1.39E-6

best growth inhibition activity with GI50 values of 319 nM and 608 nM against the leukemia cell lines SR and K-562, while NHC-AuSR showed lower activity of 663 nM and 1.62 μM on the same cell lines. Particularly interesting is the high activity of NHC-AuCl and NHC-AuSR against the prostate cancer cell line PC3 with GI50 values of 1.84 μM and 1.83 μM and the breast cancer line MDA-MB-468, for which GI50 values of 1.39 μM and 1.54 μM were determined. NHC-AuCl and NHC-AuSR showed lower activity against the multidrug-resistant ovarian cancer cell line NCI/ADR-RES with GI50 values of 3.49 μM and 5.21 μM. The activity of NHC-AuCl and NHC-AuSR is also high against the renal cell line CAKI-1 with GI50 values of 1.74 μM and 2.00 μM and therefore CAKI-1 was chosen for the xenograft *in vivo* experiment. All cell test results of NHC-AuCl and NHC-AuSR are summarised in Tables **1** and **2**.

Table 2. Overview on results obtained in cytotoxicity tests of NHC-AuSR against the NCI 60 cancer cell line panel; efficacy is shown as growth inhibition 50% (GI50) values.

Cell Line	GI50 [M]	Cell Line	GI50 [M]
Leukemia			
CCRF-CEM	1.99E-6	**NSC Lung Cancer**	
HL-60(TB)	2.24E-6	A549/ATCC	3.81E-6
K-562	1.62E-6	HOP-62	2.18E-6
MOLT-4	3.06E-6	HOP-92	1.74E-6
RPMI-8226	1.90E-6	NCI-H226	3.00E-6
SR	6.63E-7	NCI-H23	2.13E-6
		NCI-H322M	2.77E-6
		NCI-H460	2.09E-6
		NCI-H522	1.58E-6
Colon Cancer			
COLO 205	1.99E-6	**CNS Cancer**	
HCC-2998	1.96E-6	SF-268	1.88E-6
HCT-116	1.64E-6	SF-295	2.34E-6
HCT-15	1.47E-6	SF-539	1.85E-6
HT29	1.82E-6	SNB-19	1.98E-6
KM12	2.09E-6	SNB-75	1.37E-6
SW-620	1.87E-6	U251	1.61E-6
Melanoma			
LOX IMVI	1.90E-6		
MALME-3M	1.77E-6	**Ovarian Cancer**	
M14	1.69E-6	IGROV1	2.05E-6
MDA-MB-435	1.66E-6	OVCAR-3	1.61E-6
SK-MEL-2	1.74E-6	OVCAR-4	1.40E-6
SK-MEL-28	1.64E-6	OVCAR-5	1.92E-6
SK-MEL-5	1.79E-6	OVCAR-8	2.61E-6
UACC-257	1.84E-6	NCI/ADR-RES	5.21E-6
UACC-62	1.76E-6	SK-OV-3	3.39E-6
Renal Cancer		**Prostate Cancer**	
786-0	1.69E-6	PC-3	1.83E-6
A498	2.06E-6	DU-145	1.89E-6
ACHN	1.82E-6		
CAKI-1	2.00E-6	**Breast Cancer**	
RXF 393	1.63E-6	MCF7	1.55E-6
SN12C	2.22E-6	HS 578T	2.51E-6
TK-10	1.86E-6	BT-549	1.86E-6
UO-31	1.95E-6	MDA-MB-468	1.54E-6

NHC-AuCl and NHC-AuSR Mediated Growth Inhibition on CAKI-1 Xenograft Tumors

In the mouse experiment for determination of MTD eight groups of female NMRI:nu/nu mice (n=2 mice per group) were treated with single doses of 1, 5, 10 and 20 mg/kg (NHC-AuCl) or 1.5, 7.5, 15 and 30 mg/kg (NHC-AuSR). In general both compounds were tolerated by the animals. Only at higher dosage groups of 10 and 20 mg/kg NHC-AuCl animals showed abdominal swelling, and some body weight loss particularly in groups of 7.5, 15 and 30 mg/kg NHC-AuSR. These losses however were reversible and no animal died during the treatments. In these high dosage groups some liver degeneration and lighter forms of splenomegaly oc-

Table 3. Overview on results obtained in the CAKI-1 xenograft experiment. Female NMRI nu/nu mice received subcutaneous tumor cell injections on day 0. Starting at palpable tumor size the mice were treated with NHC-AuCl, NHC-AuSR or solvent at days 7, 11, 15, 22, 25 and 28. Tumor size in the treated group in relation to the control group (T/C) was measured as a therapeutic marker, while the number of deaths and the body weight change were used as toxicity parameters.

Group	Number of Mice	Substance	Treatment [on day]	Route	Dose (mg/kg)	Opt. T/C [on day]	Deaths [on day]
A	6	Solvent	7,11,15,22,25,28	i.p.			0/6
B	6	NHC-AuCl	7,11,15,22,25,28	i.p.	10	0.47 [19]	0/6
C	6	NHC-AuSR	7,11,15,22,25,28	i.p.	7.5	0.47 [29]	0/6

curred most possibly caused by abdominal accumulation of the two compounds tested. This indicates poor resorption and/or solubility of the compounds in its here used formulation, which could limit its antitumoral activity in therapeutic studies. From these investigations doses of 10 (NHC-AuCl) and 7.5 (NHC-AuSR) mg/kg were derived for a further therapeutic experiment with an extended treatment period for the tumor-bearing mice.

In the CAKI-1 s.c. tumor xenograft experiment all tumors grew progressively and the tumors reached a palpable size of around 0.1 cm^3 on day 7. Therefore, three groups of 6 mice each were treated at days 7, 11, 15, 22, 25 and 28 intraperitoneally with solvent (group A), NHC-AuCl (group B) or NHC-AuSR solution (group C). None of the mice died during the treatment; the treated mice from groups B and C showed no body weight loss when compared to the mice of the untreated group A; in all three groups the mean body weight per mouse increased continuously from around 27 g at the start to around 30 g at the end of the therapeutic experiment. Fig. **2A** shows the body weight development of the three groups during the experiment, while all parameters of the CAKI-1 xenograft experiment are shown in Table **3**.

As shown in Fig. **2B**, in both treatment groups B and C showed a tumor volume decrease after the first treatment on day 7 and reached on day 11 mean tumor volumes of 0.066 cm^3 (group B) and 0.062 cm^3 (group C), while the control cohort showed continued tumor growth and reached a significantly higher tumor volume of 0.129 cm^3. After that, treatments were given on day 11 and 15 and the tumors grew slowly but steadily at almost the same rate until day 21 when they reached mean tumor volumes of 0.102 cm^3 (group B) and 0.121 cm^3 (group C), while the control cohort reached a higher tumor volume of 0.163 cm^3. On day 29 after further 3 injections the tumors in the treated groups showed slightly increased volumes of 0.151 cm^3 (group B) and 0.149 cm^3 (group C) when the control group exhibiting a value of 0.317 cm^3. No further injections were given in the experiment and on day 35 tumor volumes of 0.189 cm^3 (group B) and of 0.167 cm^3 (group C) were measured. By contrast the solvent treated control group A reached a tumor volume of 0.345 cm^3 on day 35. Optimal T/C values of 0.47 were observed for both groups B and C on day 19 for NHC-AuCl and on day 29 for NHC-AuSR.

NHC-AuCl and NHC-AuSR Effects on Ki-67 Expression in CAKI-1 Tumors

The expression of the proliferation marker Ki-67 was quantified by immunohistochemistry in all tumors (n=6) of each group. Group A (solvent) gave an area of Ki-67 cells of 3.3 ± 0.9%, while the treatment groups B and C exhibited values of 2.1 ± 1.3% and 2.7 ± 0.9%. The ratio of Ki-67 positive cells in the solvent-treated tumors did not differ with statistical significance from those determined in the NHC-AuCl and NHC-AuSR treated groups indicating that treatment did not influence Ki-67 expression in this CAKI-1 tumor model and that these drugs do not act *via* proliferation inhibition.

NHC-AuCl and NHC-AuSR Effects on CD31 Expression in CAKI-1 Tumors

The microvessels (mv) within the control and NHC-AuCl and NHC-AuSR treated tumors were analysed by the specific CD31 staining. The CD31 positive brown-stained mv were quantified and counted by computer-based analysis in the 6 tumors of each group. The mv area measured in pixel counts (group A: 11600 ± 4300/ group B: 12300 ± 5300/ group C: 13100 ± 3800), mv mean size, which is also measured in pixel counts, (group A: 57 ± 3/ group B: 53 ± 4/ group C: 56 ± 3) and mv ratio in % (group A: 0.79 ± 0.25/ group B: 0.85 ± 0.36/ group C: 0.93 ± 0.33) remained practically unaltered. Only the mv number (group A: 38 ± 11/ group B: 27 ± 15/ group C: 25 ± 8) were decreased slightly during the gold-based treatment, but the differences were statistically not significant. This indicates that the anti-angiogenic activity of NHC-AuCl and NHC-AuSR was mild or non-existing at the dosages and treatment schedules used in the xenograft experiment.

NHC-AuCl and NHC-AuSR Effects on Inhibition of Mammalian TrxR

The inhibition of mammalian TrxR through NHC-AuCl and NHC-AuSR is significant and reaches IC50 values of 1.5 ± 0.2 μM and 3.1 ± 0.4 μM, respectively. This is significantly weaker than the inhibition of Auranofin with an IC50 value of 90 nM [38], but compares well to other NHC-Au-X complexes, which have typical values in the single digit micromolar region [39].

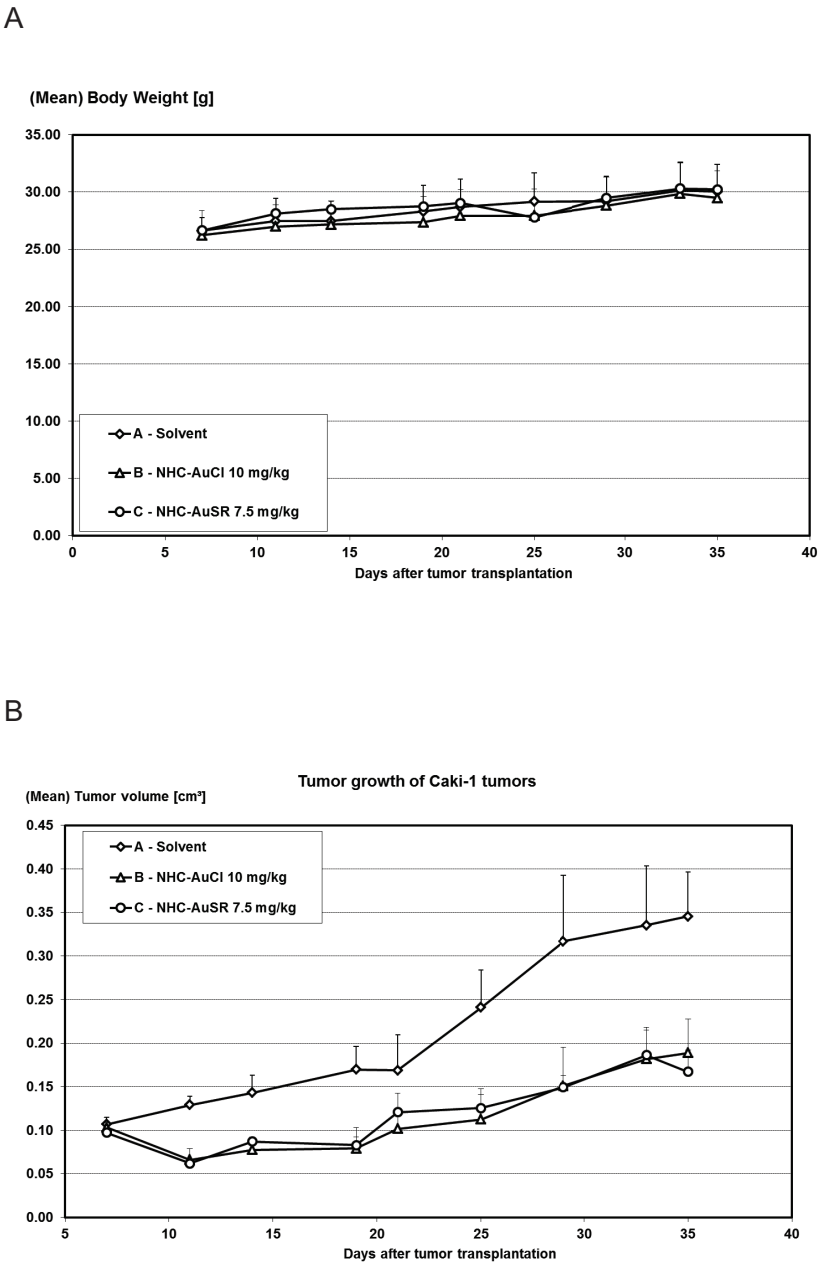

Fig. (2). Influence of NHC-AuCl and NHC-AuSR on body weight (A) and growth of CAKI-1 xenotransplant tumors (B) in NMRI nu/nu mice; the standard deviations are given as SEM.

COMPUTATIONAL RESULTS

The recently published crystal structure of GLUT1 [37] contained a *n*-nonyl-β-D-glucopyranoside ($C_{15}H_{30}O_6$) molecule (BNG), which is located inside GLUT1 as a ligand for this transporter protein. Then docking studies were performed in order to reproduce the binding mode of BNG within the GLUT1 transporter. For this purpose, BNG has been separated and then docked on the active site of GLUT1. The results showed that at least two positions match the crystal structure with binding affinities of -8.3 and -7.7 kcal/mol and that the root-mean-square deviation (RMSD) of all atoms with respect to the crystal structure are 1.099 and 0.755 Å. All binding affinity studies are summarised in Table **4**.

In the next step, NHC-Cu-thioglucoside and NHC-Au-thioglucoside with removed acetate protecting groups were docked into the GLUT1 crystal structure. Unfortunately, gold atoms are not yet parameterised in AutoDock Vina 1.1.2, and therefore direct binding energies could not be obtained. However, two docking experiments were performed in order to estimate whether the NHC-Au-thioglucoside is able to bind into GLUT1. Firstly, NHC-Cu-thioglucoside was docked successfully into GLUT1 using the optimised geometry from quantum level optimisation. Secondly, the structure of NHC-Au-thioglucoside was optimised at quantum level and the Au atom was replaced by a Cu atom keeping the C-Au and Au-S distance frozen. Rigid structure

Table 4. Binding affinities [kcal/mol] for *n*-nonyl-β-D-glucopyranoside (BNG), NHC-Cu-thioglucoside (Cu) and NHC-Au-thioglucoside with Au replaced by Cu [Au(Cu)] docked into GLUT1.

	BNG	Cu^R	Cu^F	$Au(Cu)^R$	$Au(Cu)^F$
1	-9.0	-10.4	-10.4	-10.4	-10.4
2	-8.3	-10.3	-10.4	-9.3	-10.2
3	-8.2	-9.9	-10.4	-9.1	-10.1
4	-8.0	-9.8	-10.3	-8.7	-10.1
5	-7.9	-9.7	-10.2	-8.1	-10.0
6	-7.9	-9.5	-10.1	-8.1	-10.0
7	-7.7	-9.1	-9.8	-	-9.9
8	-7.6	-8.9	-9.8	-	-9.7
9	-7.6	-8.6	-9.8	-	-9.6

R= Rigid structure, F= Flexible structure allowing rotation of all single bonds

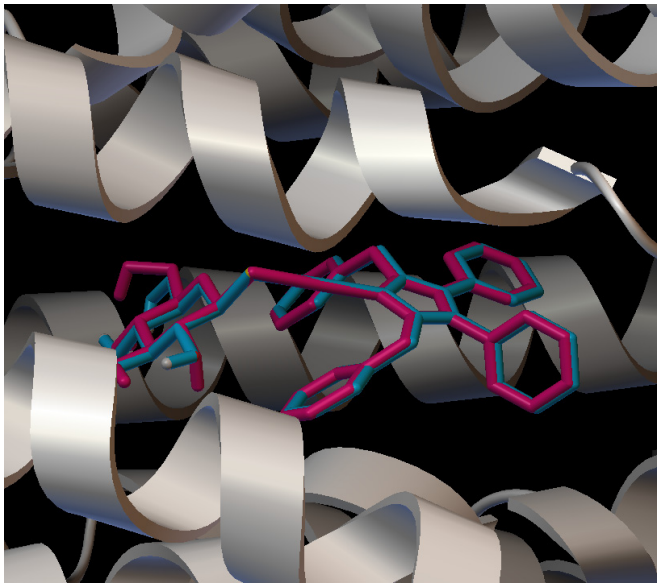

Fig. (3). Superimposed NHC-Cu-thioglucoside (magenta) and NHC-Au(Cu)-thioglucoside (blue) inside the crystal structure of human glucose transporter, GLUT1, (PDBID 4PYP).

docking as well as flexible structure docking allowing free rotation of single bonds was then performed with success. For NHC-Cu-thioglucoside both docking methods gave similar range of binding affinities with binding energies as high as 10.4 kcal/mol; all docking results are shown in Table **4**. It is observed that the NHC-Cu-thioglucoside is accommodated inside the GLUT1 with the glucoside moiety located very well when compared to BNG in the crystal structure. For the NHC-Au-thioglucoside replacement of the Au atom by an isoelectronic Cu atom was necessary. Although Cu is smaller than Au, this docking provided a good approximation of the binding affinity, since the main interaction within the GLUT1 comes from the glucoside moiety and the phenyl and benzyl groups of the NHC ligand. However, these NHC-Au(Cu)-thioglucoside binding affinities are qualitative and for comparative purposes only.

As shown in Table **4**, binding energies resulting from the docking of NHC-Au(Cu)-thioglucoside are very similar than those for NHC-Cu-thioglucoside and an identical best binding energy of 10.4 kcal/mol is found. In fact, the best positions of the two NHC-metal glucosides docked into GLUT1 are almost identical and shown in Fig. **3**. Despite the binding affinities can be considered qualitative, in all the cases the docked structures show that the NHC-Au-thioglucoside compound NHC-Au-SR can be accommodated into the GLUT1 cavity after losing its protection acetate groups. But it is impossible to predict from our docking studies, whether NHC-Au-SR will be actively transported through GLUT1 or not.

CONCLUSION

The experimental anticancer drug candidates NHC-AuCl and NHC-AuSR showed good cytotoxic activity against a wide range of cancer cell lines mostly at micromolar concentrations exhibiting average GI50 values of 1.78 and 1.95 μM, which is a good starting point for further preclinical development. Due to a long-standing interest in renal cell cancer CAKI-1 cells were chosen for the *in vivo* investigations [40, 41]. From the first *in vivo* experiments using non-tumor bearing mice and single injections MTD values of 10 mg/kg and 7.5 mg/kg were determined for NHC-AuCl and NHC-AuSR. In the therapeutic xenograft experiment using CAKI-1 tumor-bearing mice this MTD values proved to be effective and of low toxicity. When exposed to 6 dosages of 10 or 7.5 mg/kg of NHC-AuCl or NHC-AuSR none out of 6 mice died during the treatment, while identical good T/C values of 0.47 were reached on day 19 or day 29. Such activity compares well with other gold-based drugs tested *in vivo* recently [42, 43]. This treatment demonstrated that NHC-AuCl and NHC-AuSR have a useable therapeutic index in its given formulation. Particularly surprising is the fact that both compounds show only a mild or no influence on the proliferation marker Ki-67 and the angiogenesis marker CD31, but a significant effect as TrxR inhibitors killing cancer cells through enhanced oxidative stress. In addition, it was possible to show through computational methods that NHC-AuSR is a

potential ligand for glucose transporter 1 [44], which are overexpressed in many tumors. The high anti-proliferative activity of NHC-AuCl may be caused by the by the "halogen effect" found in other halogenated anticancer drug candidates like pyrimidines [45]. Therefore, NHC-AuCl and NHC-AuSR are promising anticancer drug candidates for clinical testing in the nearby future.

CONFLICT OF INTEREST

The authors confirm that this article content has no conflict of interest.

ACKNOWLEDGEMENTS

The authors gratefully acknowledge UCD and COST CM1105 for funding. The authors are thankful for the excellent technical support of B. Büttner and S. Gromova with respect to the xenograft experiments and acknowledge Dr. M. Nayel and Prof. D. Smallwood for performing the NCI 60 cell tests. Goar Sánchez-Sanz thanks Human Frontier Science Program (LT001022/2013-C) for the financial support, the Irish Centre for High-End Computing (ICHEC) for the provision of computational facilities and support and Cristina Trujillo for her useful comments and discussion. None of the authors has a commercial interest in developing NHC-AuCl or NHC-AuSR as drugs.

DISCLOSURE

This manuscript is part of a series of publications (all in LDDD) testing metal-based drug candidates against CAKI-1 derived renal-cell cancer.

REFERENCES

[1] Surveillance Epidemiology and End Results. National Cancer Institute 2007. www.seer.cancer.gov. (Accessed June 20, 2016).

[2] Schrader, A. J.; Hofmann, R. Metastatic renal cell carcinoma: recent advances and current therapeutic options. *Anti-Cancer Drugs,* **2008**, *19*, 235-245.

[3] Tan, S. J.; Yan, Y. K.; Lee, P.P.F.; Lim, K. H. Copper, gold and silver compounds as potential new anti-tumor metallodrugs. *Future Med. Chem.*, **2010**, *2*, 1591-1608.

[4] Medvetz, D. A.; Hindi, K. M.; Panzner, M. J.; Ditto, A. J.; Yun, Y. H.; Youngs, W. J. Anticancer Activity of Ag(I) N-Heterocyclic Carbene Complexes Derived from 4,5-Dichloro-1H-Imidazole. *Metal-Based Drugs*, **2008**, *7*.

[5] Patil, S. A.; Patil, S. A.; Keri, R. S.; Budagumpi, S.; Balakrishna, G.; Tacke, M. N-Heterocyclic Carbene Metal Complexes as Bioorganometallic Antibacterial and Anticancer Drugs. *Future Med. Chem.*, **2015**, *7*, 1305-1333.

[6] Tacke, M. Benzyl-Substituted Carbene-Metal Complexes: Potential for Novel Antibiotics and Anticancer Drugs? *J. Organomet. Chem.*, **2015**, *782*, 17-21.

[7] Tacke, M. Novel Carbene-Metal Complexes as Anticancer Drugs and Antibiotics-Potential and Limitations. *Insights into Coordination, Bioinorganic and Applied Inorganic Chemistry*. Melník, M.; Segľa, P.; Tatarko, M. Ed.; Press of Slovak University of Technology, Bratislava, **2015**, pp. 188-198.

[8] Browne, N.; Hackenberg, F.; Streciwilk, W.; Tacke, M.; Kavanagh, K. Assessment of Antimicrobial Activity of the Carbene Silver(I) Acetate Derivative SBC3 using Galleria Mellonella Larvae. *Biometals*, **2014**, *27*, 745-752.

[9] Hackenberg, F.; Tacke, M. Benzyl-Substituted Metallocarbene Antibiotics and Anticancer Drugs. *Dalton Trans.*, **2014**, *43*, 8144-8153.

[10] Streciwilk, W.; Cassidy, J.; Hackenberg, F.; Müller-Bunz, H.; Paradisi, F.; Tacke, M. Synthesis, cytotoxic and antibacterial studies of p-benzyl-substituted NHC-silver(I) acetate compounds derived from 4,5-p-diisopropylphenyl-or 4,5-di-p-chlorophenyl-1H-imidazole. *J. Organomet. Chem.*, **2014**, *749*, 88-99.

[11] Hackenberg, F.; Müller-Bunz, H.; Smith, R.; Streciwilk, W.; Zhu, X.; Tacke, M. Novel Ruthenium(II) and Gold(I) NHC complexes: Synthesis, characterisation and evaluation of their anticancer properties. *Organometallics*, **2013**, *32*, 5551-5560.

[12] Hackenberg, F.; Lally, G.; Müller-Bunz, H.; Paradisi, F.; Quaglia, D.; Streciwilk, W.; Tacke, M. Synthesis and biological evaluation of N-heterocyclic carbene-silver(I) acetate complexes derived from 4,5-ditolyl-imidazole. *Inorg. Chim. Acta.*, **2013**, *395*, 135-144.

[13] Sharkey, M. A.; O'Gara, J.P.; Gordon, S.V.; Hackenberg, F.; Healy, C.; Paradisi, F.; Patil, S.; Schaible, B.; Tacke, M. Investigations into the Antibacterial Activity of the Silver-Based Antibiotic Drug Candidate SBC3. *Antibiotics*, **2012**, *1*, 25-28.

[14] Hackenberg, F.; Lally, G.; Müller-Bunz, H.; Paradisi, F.; Quaglia, D.; Streciwilk, W.; Tacke, M. Novel symmetrically p-benzyl-substituted 4,5-diaryl-imidazole N-heterocyclic carbene-silver(I) acetate complexes – synthesis and biological evaluation. *J. Organomet. Chem.*, **2012**, *717*, 123-134.

[15] Hackenberg, F.; Deally, A.; Lally, G.; Malenke, S.; Müller-Bunz, H.; Paradisi, F.; Patil, S.; Quaglia, D.; Tacke, M. Novel non-symmetrically p-benzyl-substituted (benz)imidazole N-heterocyclic carbene-silver(I) acetate complexes – synthesis and biological evaluation. *Int. J. Inorg. Chem.*, **2012**, *13*.

[16] Kaps, L.; Biersack, B.; Müller-Bunz, H.; Mahal, K.; Münzner, J.; Tacke, M.; Mueller, T.; Schobert, R. Gold(I)-NHC complexes of antitumoral diarylimidazoles: structures, cellular uptake routes and anticancer activities. *J. Inorg. Biochem.*, **2012**, *106*, 52-58.

[17] Patil, S.; Deally, A.; Hackenberg, F.; Kaps, L.; Müller-Bunz, H.; Schobert, R.; Tacke, M. Novel Benzyl-or 4-Cyanobenzyl-Substituted N-Heterocyclic (Bromo)(carbene)silver(I) and (Carbene)(chloro)gold(I) Complexes: Synthesis and Preliminary Cytotoxicity Studies. *Helv. Chim. Acta.*, **2011**, *94*, 1551-1562.

[18] Patil, S.; Tacke, M. NHC-Silver(I) Acetates as Bioorganometallic Anticancer and Antibacterial Drugs. *Insights into Coordination, Bioinorganic and Applied Inorganic Chemistry*. Melník, M.; Segľa, P.; Tatarko, M. Ed.; Press of Slovak University of Technology, Bratislava, **2011**, pp. 555-566.

[19] Patil, S.; Deally, A.; Gleeson, G.; Hackenberg, F.; Müller-Bunz, H.; Paradisi, F.; Tacke, M. Synthesis, Cytotoxicity and Antibacterial Studies of Novel Symmetrically and Non-Symmetrically p-Nitrobenzyl-Substituted N-Heterocyclic Carbene-Silver(I) Acetate Complexes. *Z. Allg. Anorg. Chem.*, **2011**, *637*, 386-396.

[20] Patil, S.; Deally, A.; Gleeson, B.; Müller-Bunz, H.; Paradisi, F.; Tacke, M. Novel Benzyl-Substituted N-Heterocyclic Carbene–Silver Acetate Complexes: Synthesis, Cytotoxicity and Antibacterial Studies. *Metallomics*, **2011**, *3*, 74-88.

[21] Patil, S.; Dietrich, K.; Deally, A.; Gleeson, B.; Müller-Bunz, H.; Paradisi, F.; Tacke, M. Synthesis, Cytotoxicity and Antibacterial Studies of Novel Symmetrically and Nonsymmetrically 4-(Methoxycarbonyl) benzyl-Substituted N-Heterocyclic Carbene-Silver Acetate Complexes. *Helv. Chim. Acta.*, **2010**, *93*, 2347-2364.

[22] Patil, S.; Deally, A.; Gleeson, B.; Müller-Bunz, H.; Paradisi, F.; Tacke, M. Synthesis, Cytotoxicity and Antibacterial Studies of Symmetrically and Non-Symmetrically Benzyl-or p-Cyanobenzyl-Substituted N-Heterocyclic Carbene-Silver Complexes. *Appl. Organomet. Chem.*, **2010**, *24*, 781-793.

[23] Patil, S.; Claffey, J.; Deally, A.; Gleeson, B.; Hogan, M.; Menéndez Méndez, L.M.; Müller-Bunz, H.; Paradisi, F.; Tacke, M. Synthesis, Cytotoxicity and Antibacterial Studies of p-Methoxybenzyl-Substituted and Benzyl-Substituted N-Heterocyclic Carbene-Silver Complexes. *Eur. J. Inorg. Chem.*, **2010**, 1020-1031.

[24] Fichtner, I.; Behrens, D.; Cinatl jr., J.; Michaelis, M.; Sanders, L.C.; Hilger, R.; Kennedy, B.N.; Reynolds, A.L.; Hackenberg, F.; Lally, G.; Quinn, S.J.; McRae, I.; Tacke, M. *In vitro* and *in vivo* Investigations into the Carbene Silver Acetate Anticancer Drug Candidate SBC1. *Lett. Drug Des. Discov.*, **2012**, *9*, 815-822.

[25] Streciwilk, W.; Hackenberg, F.; Müller-Bunz, H.; Tacke, M. Synthesis and cytotoxicity studies of p-benzyl substituted NHC-copper(I) bromide derivatives. *Polyhedron*, **2014**, *80*, 3-9.

[26] Walther, W.; Fichtner, I.; Hackenberg, F.; Streciwilk, W.; Tacke, M. *In vitro* and *in vivo* Investigations into the Carbene Copper Bromide

Anticancer Drug Candidate WBC4. *Lett. Drug Des. Discov.*, **2014**, *11*, 825-832.

[27] Tonissen, K. F.; Di Trapani, G. Thioredoxin system inhibitors as mediators of apoptosis for cancer therapy. *Mol. Nutr. Food Res.*, **2009**, *53*, 87-103.

[28] Barnard, P.J.; Berners-Price, S.J. Targeting the mitochondrial cell death pathway with gold compounds. *Coord. Chem. Rev.*, **2007**, *251*, 1889-1902.

[29] Chan, D. A.; Sutphin, P. D.; Nguyen, P.; Turcotte, S.; Lai, E. W.; Banh, A.; Reynolds, G.E.; Chi, J.-T.; Wu, J.; Solow-Cordero, D.E.; Bonnet, M.; Flanagan, J.U.; Bouley, D.M.; Graves, E.E.; Denny, W.A.; Hay, M.P.; Giaccia, A. J. Targeting GLUT1 and the Warburg Effect in Renal Cell Carcinoma by Chemical Synthetic Lethality. *Sci. Transl. Med.*, **2011**, *3*, 94ra70.

[30] Shoemaker, R.H. The NCI60 human tumor cell line anticancer drug screen. *Nat. Rev. Cancer*, **2006**, *6*, 813-823.

[31] Becke, A.D. Density-functional thermochemistry. III. The role of exact exchange. *J. Chem. Phys.*, **1993**, *98*, 5648-5652.

[32] Lee, C.T.; Yang, W.T.; Parr, R.G. Development of the Colle-Salvetti correlation-energy formula into a functional of the electron density. *Phys. Rev. B*, **1988**, *37*, 785-789.

[33] Frisch, M.J.; Pople, J.A.; Binkley, J.S. Self-consistent molecular orbital methods 25. Supplementary functions for Gaussian basis sets. *J. Chem. Phys.*, **1984**, *80*, 3265-3269.

[34] Check C. E.; Faust T. O.; Bailey J. M.; Wright B. J.; Gilbert T. M.; Sunderlin L. S. Addition of Polarization and Diffuse Functions to the LANL2DZ Basis Set for p-Block Elements. *J. Phys. Chem. A*, **2001**, *105*, 8111-8116.

[35] Gaussian 09, Gaussian Inc., Wallingford CT, **2009**.

[36] Trott, O.; Olson, A.J. Software news and update AutoDock Vina: Improving the speed and accuracy of docking with a new scoring function, efficient optimization, and multithreading. *J. Comp. Chem.*, **2010**, *31*, 455-461.

[37] Deng, D.; Xu, C.; Sun, P.; Wu, J.; Yan, C.; Hu, M.; Yan, N. Crystal structure of the human glucose transporter GLUT1. *Nature*, **2014**, *510*, 121-125.

[38] Rubbiani, R.; Kitanovic, I.; Alborzinia, H.; Can, S.; Kitanovic, A.; Onambele, L.A.; Stefanopoulou, M.; Geldmacher, Y.; Sheldrick, W.S.; Wolber, G.; Prokop, A.; Wölfl, S.; Ott, I. Benzimidazol-2-ylidene Gold(I) Complexes Are Thioredoxin Reductase Inhibitors with Multiple Antitumor Properties. *J. Med. Chem.*, **2010**, *53*, 8608-8618.

[39] Rubbiani, R.; Schuh, E.; Meyer, A.; Lemke, J.; Wimberg, J.; Metzler-Nolte, N.; Meyer, F.; Mohr, F.; Ott, I. TrxR inhibition and antiproliferative activities of structurally diverse gold N-heterocyclic carbene complexes. *Med. Chem. Commun.*, **2013**, *4*, 942-948.

[40] Fichtner, I.; Pampillón, C.; Sweeney, N.J.; Strohfeldt, K.; Tacke, M. Antitumor Activity of Titanocene Y in Xenografted Caki-1 Tumors in Mice. *Anti-Cancer Drugs*, **2006**, *17,* 333-336.

[41] Walther, W.; Fichtner, I.; Deally, A.; Hogan, M.; Tacke, M. The Activity of Titanocene T Against Xenografted CAKI-1 Tumors. *Lett. Drug Des. Discov.,* **2013**, *10*, 375-381.

[42] García-Moreno, E.; Tomás, A.; Atrián-Blasco, E.; Gascón, S.; Romanos, E.; Rodriguez-Yoldi, M.J.; Cerrada, E.; Laguna, M. *In vitro* and *in vivo* evaluation of organometallic gold(I) derivatives as anticancer agents. *Dalton Trans.*, **2016**, *45*, 2462-2475.

[43] Fernández-Gallardo, J.; Elie, B. T.; Sulzmaier, F. J.; Sanaú, M.; Ramos, J.W.; Contel, M. Organometallic Titanocene–Gold Compounds as Potential Chemotherapeutics in Renal Cancer: Study of their Protein Kinase Inhibitory Properties. *Organometallics*, **2014**, *33*, 6669-6681.

[44] Patra, M.; Johnstone, T.C.; Suntharalingam, K.; Lippard, S. J. A Potent Glucose–Platinum Conjugate Exploits Glucose Transporters and Preferentially Accumulates in Cancer Cells. *Angew. Chem.*, **2016**, *128*, 2596-2600.

[45] Temburnikar, K.W.; Ross, C. R.; Wilson, G. M.; Balzarini, J.; Cawrse, B. M.; Seley-Radtke, K. L. Antiproliferative activities of halogenated pyrrolo[3,2-d]pyrimidines. *Bioorg. Med. Chem.*, **2015**, *23*, 4354-4363.